



## A study on the magnetic field profile associated with the solar wind

Devendra Gautam

Assistant Professor, Department of Physics, Janata College, Rewa, Madhya Pradesh, India

### Abstract

As the model magnetic cloud moves past the earth, an observe (e.g. a satellite) sees a magnetic field varying in time. In this example, the northward component ( $B_z > 0$ ) arrives at the earth first (Chen, 1996). The continued expansion in the minor radial direction is taken into account. Although no ambient magnetic field is included outside the cloud edges (the vertical dashed lines), the solar wind typically has fluctuating field of roughly 5nT in magnitude. A nonzero by outside the flux rope will cause theta (panel c) to decrease. The  $B_y$  and  $B_z$  components and theta are shown. The above theoretical model closely resembles the observed magnetic cloud. The  $B_y$  component, which is in the east-west direction, peaks where  $B_z = 0$ . The sign difference in  $B_y$  cloud wind speed  $V$  and density are also shown. The major gaps in the data are indicated by vertical dashed lines.

**Keywords:** magnetic field, solar wind, heliomagnetic, earth's

### Introduction

Earth's magnetic field is compressed due to interaction of solar wind, which creates a cavity in interplanetary space called magnetosphere, where the earth's magnetic field dominates in the magnetic field of the solar wind. The magnetosphere is shaped somewhat like a comet in response to the dynamic pressure of the solar wind. It is compressed on the side towards the sun to about 10 earth radii and is extended tail-like on the side away from the sun to more than 100 earth radii. The magnetosphere deflects the flow of most solar wind particles around the earth, while the geomagnetic field lines guide charged particle motion within the magnetosphere.

The differential flow of ions and electrons inside the magnetosphere and in the ionosphere form current system, which cause variations in the intensity of the earth's magnetic field. These external currents in the ionized upper atmosphere and magnetosphere vary on a much shorter time scale than the internal main field and may create magnetic field as large as ten percent of the main field.

It is the main field component that is modeled by the International Geomagnetic Reference Field (IGRF) and World Magnetic Model (WMM). Other important sources are the fields arising from electrical currents flowing in the ionized upper atmosphere, and the fields induced by currents flowing within the earth's crust. The main field component varies slowly in time and can be grossly described as that of a bar magnet with north and south poles deep inside the earth and magnetic field lines that extend well out into space. The earth's magnetic field varies both in space and time. The geomagnetic field measured at any point on the earth's surface.

The magnetotail is a consequence of the merging of solar wind magnetic field lines with those of the earth, the latter then being stretched far down stream by the force imparted from the on flowing solar wind (Dungey, 1961)<sup>[1]</sup>. Recent

findings suggest that a force skin to viscous drag is acting on closed field lines at the magnetosphere's surface shares in the formation of magnetotail. The geomagnetic tail extends to several tens of earth radii. The boundary of the tail roughly resembles the surface of along cylinder. In the northern half of the cylinder, the field lines are roughly directed towards the sun, and in the southern half away from the sun. The plasma sheet separates the oppositely directed fields in tail lobes. The formation of the sheet begins near the magnetic equatorial plane at a geocentric distance of  $10 \pm 3$  Re. The thickness of this plasma sheet varies greatly with geomagnetic activity but is typically 5 Re. and the sheet extends most of the way down the tail. The plasma sheet surrounds a region of very weak fields, the neutral sheet where the tail field reverses. A current must flow in the neutral sheet across the tail to maintain the tail configuration of oppositely directed field lines. The electromotive force of the magnetospheric dynamo derives a current around each tail lobe and accumulates positive space charge on the dusk side. The electric current resulting from the charge separation is discharged through the crosstail current keeping the two lobes apart.

### Data analysis

Initially, the magnetic field magnitude, that a spacecraft should detect when passes through a magnetic cloud, is modelled as a static cavity. The solution of the Grad Shafranov equation for the cavity gives the behavior of the poloidal flux, which is related to the magnetic field components.

$$\psi = \sin^2 \theta \left[ C_1 \left( \alpha \cos(\pi r) - \frac{\sin(\pi r)}{r} \right) - \frac{F_0}{a^2 r^2} \right]$$

$$B_r = \frac{2 \cos \theta}{r^2 \sin^2 \theta} \frac{\partial \psi}{\partial r}$$

$$B_\theta = \frac{r \sin \theta}{\alpha} \frac{\partial \psi}{\partial r}$$

$$B_\phi = \frac{\psi}{r \sin \theta}$$

In this case the solution is given for spherical coordinates. Enforced the specific boundary conditions to a flux confined in a sphere of unit radius, the solution has three free parameters which should satisfy the conditions. For the study case, these are  $\alpha = 5.76$ ,  $F_0 = \neq 24.46$  and  $C_1 = \neq 0.13$ , which are the smallest roots (Gourgouliatos *et al.* 2011) [2].

**Interplanetary magnetic field**

Process inside the sun break its temporal and spatial homogeneity, creating an ever-changing photosphere. An important element of this spatial and temporal inhomogeneity is the presence of a magnetic field generated at the base of the convection layer that extends high into the corona and the solar wind. This magnetic field in turn affects the spherical symmetry of the solar wind expansion and suppresses that expansion in some places. Fig. 1 shows both an undisturbed dipole field and isothermal MHD coronal expansion model of Pneumann and Kopp (1971)[3]. The dipolar magnetic field in this model keeps the equatorial corona tied to the sun. At higher latitudes the solar wind expands along the magnetic field, carrying the solar wind field into interplanetary space from the polar regions of the sun and creating a heliospheric current sheet between the two polar coronal hole outflows.

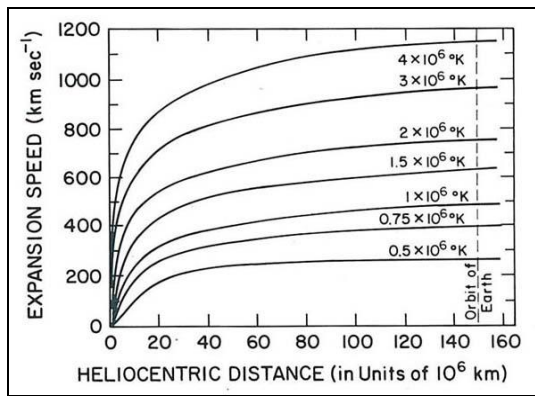


Fig 1

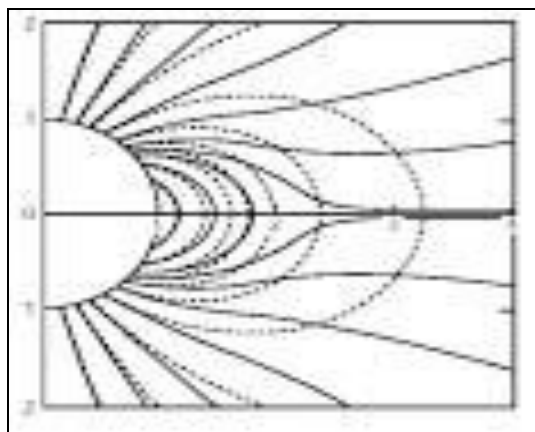


Fig. 2

The magnetic pattern is usually not symmetric about the rotational axis of the sun nor is it purely dipolar. In the latter case the heliomagnetic equator that separates inward and outward interplanetary magnetic field is warped. Thus, as the

sun rotates, the pattern set by the sun's field sweeps over the earth causing the magnetic the magnetic sectors seen in the interplanetary magnetic field as illustrated in in 3D perspective. Furthermore, the earth's orbit is not in the rotational equator of the sun so that in the course of a year the earth spends six month above the rotational equator and six months below it.

The closed magnetic regions allow the corona to build up in density and temperature in the magnetic equatorial or streamer belt region, as sketched in Fig. 3 and as seen with the naked eye at the time of eclipses. In the coronal hole regions on the sun, from which the solar wind flows freely and whose magnetic field lines are open are called coronal holes. In these regions the density is lower and the temperature cooler. The connectivity of coronal holes and the more distant solar wind has been demonstrated by tracing field lines back to the sun with an MHD model (Linker *et al.* 1999) [4]. The model also reproduces the intensity variations seen in the streamer belt of the lower corona and has been used to predict the appearance of the sun during total solar eclipses.

Since the streamer belt is nearly equatorial at least at solar minimum, the slow solar wind is an average found near the ecliptic plane and the fast solar wind at high latitudes. Ulysses measurements out of the ecliptic plane (McComas *et al.* 1998) [5] and shown in the accompanying paper by Gosling (1996) [6] emphasize what a biased sample the earth receives of the solar wind.

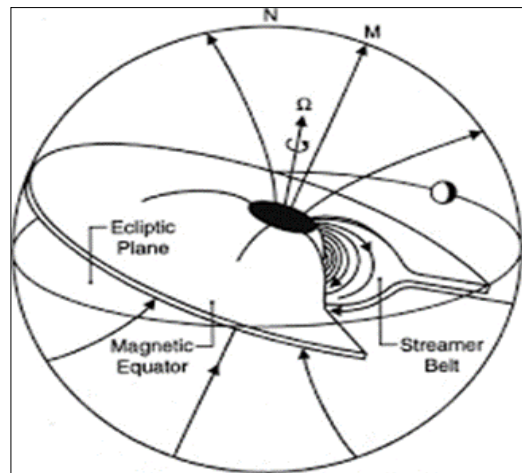


Fig 3

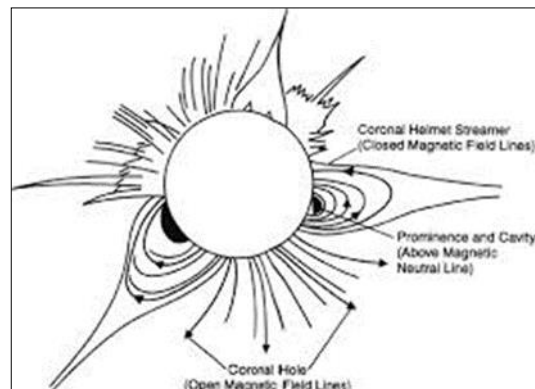


Fig 4

However, even though solar wind properties such as composition are ordered by the solar wind speed this control appears as a continuous change and there is no sudden change in properties at some particular speed. Again using MHD models to extrapolate the solar wind back to its solar source puts the origin of the fast solar wind in coronal holes (Neugebauer *et al.* 1998) [7]. A corollary of this magnetic control of the solar wind expansion is that the flux tube divergence of the magnetic field measured at the source surface correlates well but negatively with the solar wind speed (Wang and Sheeley, 1990) [8]. Where coronal magnetic flux tubes are straight and radial the solar wind is fast and where they strongly diverge the solar wind is slow. During solar maximum coronal holes and regions of flux tube divergence are more evenly spread over the Sun's surface than at solar minimum, allowing the earth to experience a broad range of solar wind velocities, almost independent of its heliographic or heliomagnetic latitude. During the declining phase of solar activity when the current sheet has a large tilt to the solar equator but there is more order to the coronal fields, a more stable fast/slow stream structure arises. It is possible that some slow solar wind arises in the coronal streamer belt (Gosling *et al.* 1997) [9] but this source is not expected to provide as steady or as wide a region of slow solar wind as that observed.

### Conclusion

The technique takes advantage of the fact that the solar wind (SW) features that cause large storms, long uninterrupted durations of strong southward or northward magnetic field, make such geoeffective structures clearly distinguishable from the non geoeffective ("background") solar wind. They can be described as magnetic flux ropes propagating past the earth. If the magnetic field of an interplanetary flux rope is measured, the field vector shows a characteristic rotation which is much slower than the time scale of IMF fluctuations in the background solar wind. The slow rotation of the magnetic field can be recognized and used to infer the magnetic field profile of the solar wind that has yet to arrive at the earth. This means that the leading edge of the SW structure has a structural relationship to the trailing edge. The basic technique falls under the broad category of artificial intelligence. Another artificial intelligence approach uses neural networks and a number of neural network space weather forecasting techniques are under development elsewhere. The basic difference is that our technique seeks to estimate the magnetic field profile (Bz) forward in time, in the solar wind that has yet to arrive at the observing platform. The response of the magnetosphere to the predicted Bz profile is then inferred. In contrast, the neural network approach attempts to predict the response of the magnetosphere to the solar wind that has been observed.

Because the earth passage of magnetic clouds takes 10-20 hours to a few days, the method allows prediction of IMF forward in time. As a result, the method can yield advance forecasting time of several to more than 10 hours. This is far in excess of the warning time achieved by the current neural network techniques which attempt to predict the response of the magnetosphere to the measured solar wind data (Chen *et al.* 1996-1997) [10].

The test is being conducted to examine the degree of success one can expect from the method in its present form with respect to the following specified objectives. The first is to estimate the eventual duration  $\tau$  and maximum value of Bz field (denoted  $B_{zm}$ ) of each solar wind event being encountered. The second objective is to estimate the Bz(t) profile of the solar wind stream that has yet to come. The third objective is to determine whether the event is geoeffective or not geoeffective according to the estimated  $B_{zm}$  and  $\tau$ . The threshold for geoeffectiveness is chosen to be  $Dst < -80nT$  for two hours or longer. Our overall objective is to accurately identify and predict the solar wind events that cause large geomagnetic storms rather than the detailed response of the magnetosphere. We judge the success of the technique as follows. If a solar wind event leads to  $P1 > 0.5$  for 2 hours or longer, we regard the outcome as a positive prediction of the occurrence of  $Dst < -80nT$ . We then compare this outcome with the actual or provisional Dst value, whichever may be available. If Dst does fall and remain below this threshold for two hours or longer, the prediction is judged to be correct. If P1 does not exceed 0.5 for two hours or longer but Dst does fall below the -80nT Threshold, then the result is judged to be a false negative (a miss). If P1 produces a positive prediction for storm but Dst does not fall below the -80nT threshold, the outcome is judged to be a false positive (a false alarm). The association between the solar wind events and the Dst values can be subjective, but we generally do not encounter obvious ambiguity.

### References

1. Dungey JW. Interplanetary magnetic field and the auroal zones, *Phys. Rev. Lett.* 1961; 6:47-48.
2. Gourgouliatos, Konstantinos N, Maxim Lyutikov. Dynamics of rising magnetized cavities and UHECR acceleration in clusters of galaxies. *Monthly Notices of the Royal Astronomical Society.* 2011; 9:1-9.
3. Pneumann GW, Kopp RA. *Solar Phys.* 1971; 18:258.
4. Linker, *et al.* *Geophys.* in press First citation in article, 1999.
5. McComas DJ, *et al.*, Ulysses' return to the slow solar wind, *Geophys. Res. Lett.* 1998; 25:1.
6. Gosling JT. Corotating and transient solar wind flows in three dimensions, *Annu. Rev. Astron. Astrophys.* 1996; 34:35-XX.
7. Neugebauer, *et al.* *J Geophys. Res.* 1998; 103:14587.
8. Wang YM, Sheeley NR. Solar wind speed and coronal flux-tube expansion, *Astrophysical Journal, Part 1.* 1990; 355:726-732.
9. Gosling JT, Bame SJ, Feldman WC, McComas DJ, Riley P, Goldstein BE, *et al.* The northern edge of the band of solar wind variability: Ulysses at ~4.5 AU, *Geophys. Res. Lett.* 1997; 24:309.
10. Chen J. Cargill and Palmadesso, *Geophys. Res. Lett.* 1996-1997; 23:625.